OPEN

Stromal Fibrosis and Expression of Matricellular Proteins Correlate With Histological Grade of Intraductal Papillary Mucinous Neoplasm of the Pancreas

Yasuharu Kakizaki, MD, PhD, Naohiko Makino, MD, PhD,* Tomohiro Tozawa, MD, PhD,* Teiichiro Honda, MD, PhD,* Akiko Matsuda, MD, PhD,* Yushi Ikeda, MD, PhD,* Miho Ito, MD, PhD,* Yoshihiko Saito, MD,* Wataru Kimura, MD, PhD,† and Yoshiyuki Ueno, MD, PhD**

Objective: The aim of the study was to clarify the correlation between the microenvironmental factors and histological grade in intraductal papillary mucinous neoplasm (IPMN).

Methods: We investigated 65 IPMNs resected at Yamagata University Hospital between 2000 and 2011, and all cases were categorized to low-inter (including low- and intermediate-grade dysplasia) and high-inv (including high-grade dysplasia and IPMN with an associated invasive carcinoma) groups. We compared between the 2 groups pathologically with regard to fibrosis and the expression of alpha-smooth muscle actin (α-SMA), periostin, and galectin-1 in the periductal stroma of IPMN.

Results: There were 41 low-inter and 24 high-inv. The subtype was categorized as 22 main duct type (MD-IPMN) and 43 branch duct type (BD-IPMN). The degree of fibrosis and the expression of α-SMA, periostin, and galectin-1 were significantly higher in high-inv than in low-inter within BD-IPMNs. Multivariate logistic regression analysis indicated that high expression of α-SMA (odds ratio, 13.802; 95% confidence interval, 1.108–171.893; $P = 0.0414$) was a significant independent related factor of high-inv in BD-IPMN.

Conclusions: Stromal fibrosis and expression of α-SMA, periostin, and galectin-1 are more marked in high-inv than in low-inter within BD-IPMNs, and they could become new markers for determining the indications for surgery in BD-IPMN.

Key Words: intraductal papillary mucinous neoplasm, stromal fibrosis, alpha-smooth muscle actin, periostin, galectin-1

(*Pancreas* 2016;45: 1145–1152)

Intraductal papillary mucinous neoplasm (IPMN) of the pancreas was first reported as "mucin-producing cancer" in 1982[1] and named IPMN in the World Health Organization (WHO) classification in 2000.[2] For the last several decades, IPMN has been diagnosed with increasing frequency.[3] This tumor, which is a precursor lesion of pancreatic cancer, is characterized by mucin production, cystic dilation of the pancreatic duct, and slow growth. In the WHO classification of 2010, IPMN was divided pathologically into variants showing low-, intermediate-, high-grade dysplasia and IPMN had an associated invasive carcinoma.[4] Intraductal papillary mucinous neoplasm is considered to show stepwise progression of growth.[5] According to the *General Rules for the Study of Pancreatic Cancer* (6th ed) of the *Japan Pancreas Society*,[6] IPMN is divided pathologically into intraductal papillary mucinous adenoma and intraductal papillary mucinous carcinoma (noninvasive, minimally invasive, or invasive). A multi-institutional retrospective study of 1379 cases of IPMN by the *Japan Pancreas Society* indicated that the 5-year survival rate was 98% to 100% for patients with IPMNs manifesting adenoma to noninvasive carcinoma but 57.7% for those with invasive carcinoma.[7] Accordingly, surgical resection of IPMNs is considered necessary before invasion occurs.

On the basis of imaging findings and pathology, IPMNs are divided into the main duct type (MD-IPMN), the branch duct type (BD-IPMN) and the mixed type. The MD-IPMN lesions are predominantly associated with a dilated main pancreatic duct (MPD), and BD-IPMN lesions with cystic dilation of the branch duct.[8] Interestingly, the mean frequency of malignancy in MD-IPMN and the mixed type is nearly 60%, whereas that in BD-IPMN is nearly 25%. On the basis of the algorithm for follow-up and assessing the operability of IPMNs suggested by the International Consensus Guidelines 2012,[9] resection is recommended for all MD-IPMNs and the mixed type if long patient survival is expected, whereas follow-up is recommended for BD-IPMN unless there are signs of malignancy including the presence of obstructive jaundice, an enhanced solid component within the cyst, or dilatation of the MPD. This subtyping is useful for decision of operability in IPMN, although the reasons for the differences in malignancy between the subtypes remain unidentified. Furthermore, a large cyst diameter, a large MPD diameter, and a large mural nodule were known predictive factors of IPMN malignancy.[10] Because preoperative pathological diagnosis is difficult for IPMN, differential diagnosis of malignancy using the predictive factors from imaging modalities is required. However, relevant operability is still uncertain. Accordingly, credible predictive factors for IPMN malignancy are urgently needed.

Recently, activated pancreatic stellate cell (PSC), cancer-associated fibroblast, and matricellular protein have been shown to act as accelerators of pancreatic cancer. Desmoplasia involves extracellular matrix protein, immune cells, cancer-associated fibroblasts, and activated PSCs, the latter being particularly crucial for desmoplasia formation.[11–15] When activated PSCs show myofibroblast-like transformation morphologically, expressing alpha-smooth muscle actin (α-SMA)[16] and performing multiple functions such as proliferation, migration, and production of extracellular matrix proteins.[14] Therefore, persistent activation of PSCs results in desmoplasia. There is accumulating evidence to suggest that stromal-epithelial interaction, PSCs, and pancreatic cancer cells stimulate each other through growth factors (platelet-derived growth factor, transforming growth factor β_1, etc), leading to an increase of malignancy.[11–15] Furthermore, a previous report has shown that a high level of α-SMA mRNA from tissue samples of pancreatic cancer is an

From the Departments of *Gastroenterology and †Gastroenterological, General, Breast, and Thyroid Surgery, Yamagata University Faculty of Medicine, Yamagata, Japan.

Received for publication December 25, 2014; accepted December 8, 2015.

Address correspondence to: Naohiko Makino, MD, PhD, Department of Gastroenterology, Yamagata University Faculty of Medicine, 2-2-2 Iida-Nishi, Yamagata-shi, Yamagata 990-9585, Japan (e-mail: namakino@med.id.yamagata-u.ac.jp).

The authors declare no conflict of interest.

DOI: 10.1097/MPA.0000000000000617

independent prognostic factor, suggesting that PSC activation is closely related to the malignant behavior of pancreatic cancer.[17]

Cancer-associated fibroblasts are observed in the tumor-associated stroma of various cancers including those of the breast, prostate, and pancreas.[18] Activated stromal fibroblasts, such as PSCs, can be identified by their expression of α-SMA. It has been reported previously that overexpression of podoplanin in cancer-associated fibroblasts is correlated with increased migration and invasion of pancreatic cancer cells in vitro and correlated with shorter survival in patients. Accordingly, cancer-associated fibroblasts are believed to play a role in the progression of pancreatic cancer.[19]

Matricellular proteins are a group of extracellular proteins that modulate cell-matrix interactions and cellular functions.[14,15] Up-regulation of matricellular proteins, including periostin and galectin-1, has been observed in the stroma of pancreatic cancer, and it has been considered that matricellular proteins produced by PSCs promote the formation of a tumor-supportive microenvironment.[20–23]

In the light of these facts, we hypothesized that IPMN malignancy might be attributable to factors in the microenvironment around the enlarged pancreatic duct, such as stromal fibrosis (including desmoplasia), activated PSCs, activated fibroblasts, and the expression of matricellular proteins, as is the case in pancreatic cancer. Accordingly, the aim of the study was to investigate the degree of fibrosis, the expression of α-SMA, and the expression of periostin and galectin-1 as matricellular proteins in the periductal stroma of IPMN. Furthermore, we assessed the correlation between those microenvironmental factors and histological grade in IPMN.

MATERIALS AND METHODS

Tissue Samples, Clinical Parameters, and Classification

We evaluated 65 patients with IPMNs who underwent surgery including pancreatoduodenectomy, distal pancreatectomy, and total pancreatectomy at Yamagata University Hospital (Yamagata, Japan) between 2000 and 2011. All cases were diagnosed with IPMN using the imaging modalities including abdominal ultrasound, endoscopic ultrasonography, endoscopic retrograde pancreatography, contrast-enhanced computed tomography, and magnetic resonance imaging and also pathologically using hematoxylin-eosin staining. Cases showing dilation of the MPD or components of the neoplasm affecting the MPD were considered to be MD-IPMN, and cases showing mucinous cystic lesions communicated with the pancreatic duct were considered to be BD-IPMN. Mixed-type IPMN was included in the MD-IPMN group. On the basis of the WHO classification of 2010,[4] IPMNs were classified pathologically as low-, intermediate-, high-grade dysplasia and IPMN with an associated invasive carcinoma. Furthermore, the cases were divided into a low-inter group, including low- and intermediate-grade dysplasia, and a high-inv group, including high-grade dysplasia and IPMN with an associated invasive carcinoma. The present study was approved by the ethics committee of Yamagata University Faculty of Medicine on October 15, 2012.

Staining

Three to 5 formalin-fixed, paraffin-embedded tissue blocks containing the enlarged pancreatic duct were selected for each case and cut into sections 3-μm thick, followed by staining with hematoxylin eosin. Masson trichrome staining (Sigma-Aldrich Japan, Tokyo, Japan) was performed for evaluation of fibrosis, as reported previously. Immunohistochemistry was performed to evaluate the expression of α-SMA, periostin, and galectin-1. For this purpose, the sections were deparaffinized and heated in citrate buffer for 20 minutes in a microwave oven. Endogenous peroxidase was blocked using 0.3% hydrogen peroxide in methanol for 30 minutes at room temperature. After incubation with each primary antibody at 4°C overnight, the sections were incubated with the biotinylated secondary antibody for 30 minutes at room temperature and reacted with a Vectastain ABC kit (Vector Laboratories, Burlingame, Calif), with the exception of periostin for which a Vectastain Elite ABC kit (Vector Laboratories) was used. The immunoreaction was colored with 3,3′-diaminobenzidine substrate (Muto Pure Chemicals, Tokyo, Japan) and counterstained with hematoxylin. The primary antibodies and dilutions employed were the following: anti–α-SMA (M0851; DAKO Japan, Tokyo, Japan, 1:50), antiperiostin (RD181045050; BioVendor, Brno Czech Republic, 1:4000), and antigalectin-1 (sc-166618; Santa Cruz Biotechnology, Dallas, Tex, 1:40). For the negative control, the nonspecific IgG antibody (including Negative Control Mouse IgG2a, X0943, and Rabbit Immunoglobulin Fraction, X0903; DAKO Japan) was used, and this was confirmed to elicit no immunoreactivity.

Evaluation

A Carl Zeiss Axio Observer D1 Inverted Microscope (Carl Zeiss Japan, Tokyo, Japan) was used for observation of the specimens at magnifications of ×50, ×100, or ×200, and 10 visual fields containing the enlarged pancreatic duct were selected arbitrarily from each case at a magnification of ×50 (2402161.63 μm^2 for 1 field). The degree of fibrosis was calculated as the total fibrotic area in 10 selected fields divided by the total area of tissue stained with Masson trichrome, and the rate of immunopositivity was calculated as the total area positively stained in the same 10 selected fields divided by the total tissue area. AxioVision 4.7.1 (Carl Zeiss) was used for calculation of area.

TABLE 1. Characteristics of Patients With IPMN (N = 65)

Age, median (range), y	69 (39–87)
Sex, n (%)	
Male	47 (72.3)
Female	18 (27.7)
BMI, median (range)	21.3 (15.4–36.3)
Pathology, n (%)	
Low-inter group	41 (63.1)
High-inv group	24 (36.9)
Subtype, n (%)	
MD-IPMN	22 (33.8)
BD-IPMN	43 (66.2)
Cyst diameter, median (range), mm	32.2 (16.0–90.0)
MPD diameter, median (range), mm	5.0 (1.9–40.0)
Mural nodule size, median (range), mm	0.0 (0.0–20.0)
Serum CEA, median (range), ng/mL	2.40 (0.49–26.92)
Serum CA19-9, median (range), U/mL	10.90 (0.60–1973.20)
Fasting plasma glucose, median (range), mg/dL	98.0 (74.0–160.0)
HbA1c (JPN), median (range), %	5.4 (3.6–8.3)
Serum amylase, median (range), U/L	77.0 (37.0–273.0)
Serum lipase, median (range), U/L	30.0 (6.0–159.0)

HbA1c (National Glycohemoglobin Standardization Program) is almost equivalent to HbA1c (JPN) + 0.4%. HbA1c (JPN) was used until 2010 in Japan Diabetes Society.

CA indicates carbohydrate antigen; CEA; carcinoembryonic antigen; high-inv group, IPMN with high-grade dysplasia and IPMN with an associated invasive carcinoma; low-inter group, IPMN with low- and intermediate-grade dysplasia.

Statistical Analysis

Statistical analysis was performed using SAS Enterprise Guide 4.3 (SAS Institute Inc., Cary, NC). Graphs were prepared using Excel 2007. Student *t* test was used for comparison of quantitative data in 2 groups with a normal distribution. The Mann-Whitney *U* test was used for comparison of quantitative data in 2 groups without a normal distribution. The χ^2 test or Fisher exact test was used for comparison of categorical data in 2 groups. Logistic regression analysis was used for univariate and multivariate analyses. The level of statistical significance was set at a *P* value of less than 0.05 and 0.01.

RESULTS

Characteristics of Patients with IPMN

The median (range) age of all IPMNs was 69 (39–87) years. There were 47 men and 18 women. The pathology of IPMN was categorized as either the low-inter group (n = 41) or the high-inv group (n = 24). The subtype was categorized as either MD-IPMN (n = 22) or BD-IPMN (n = 43). The median (range) of cyst diameter, MPD diameter, and mural nodule size were 32.2 (16.0–90.0) mm, 5.0 (1.9–40.0) mm, 0.0 (0.0–20.0) mm, respectively. The cyst diameter was calculated by the data of the BD-IPMN and the mixed-type IPMN (Table 1).

Pathology

All IPMNs were subjected to staining with hematoxylin-eosin and Masson trichrome, as well as immunohistochemistry for α-SMA, periostin, and galectin-1.

Observation of BD-IPMN with low-grade dysplasia at a magnification of ×50 showed that the fibrotic band in the stroma surrounding the enlarged pancreatic duct was narrow (Fig. 1A1) and that the stroma was immunoreactive for α-SMA, periostin, and galectin-1 (Fig. 1A2–A4). At ×200, diffuse immunoreactivity of α-SMA was observed in the fibrotic band, whereas

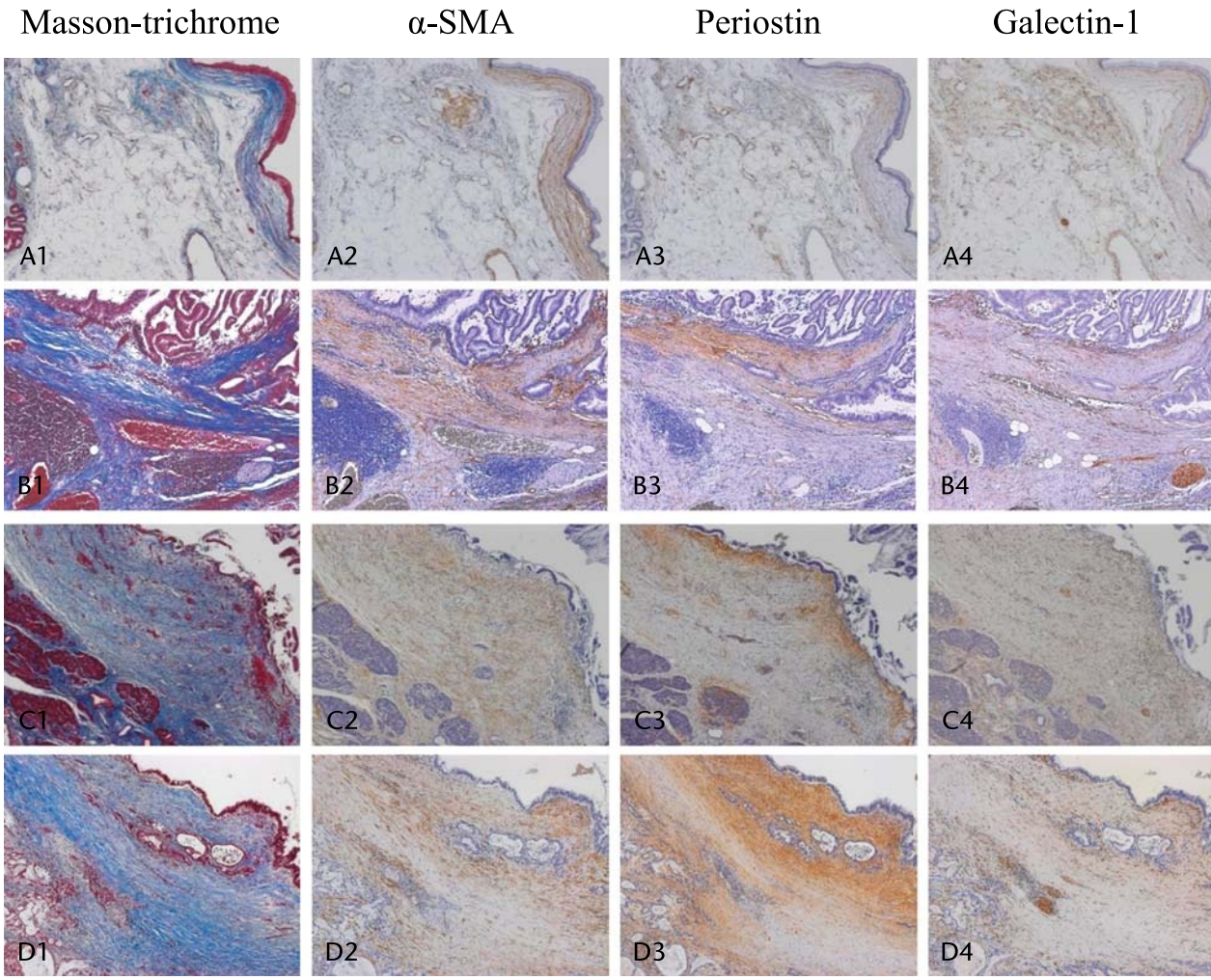

FIGURE 1. Pathology of IPMN. A1–A4, Pathology of BD-IPMN with low-grade dysplasia stained with Masson trichrome (A1) and using immunohistochemistry for α-SMA (A2), periostin (A3), and galectin-1 (A4) at a magnification of ×50. B1–B4, Pathology of BD-IPMN with high-grade dysplasia stained with Masson trichrome (B1) and using immunohistochemistry for α-SMA (B2), periostin (B3), and galectin-1 (B4) at ×50. C1–C4, Pathology of MD-IPMN with low-grade dysplasia stained with Masson trichrome (C1) and using immunohistochemistry for α-SMA (C2), periostin (C3), and galectin-1 (C4) at ×50. D1–D4, Pathology of MD-IPMN with an associated invasive carcinoma stained with Masson trichrome (D1) and using immunohistochemistry for α-SMA (D2), periostin (D3), and galectin-1 (D4) at ×50. Fibrosis and the immunoreactivity for α-SMA, periostin, and galectin-1 in the periductal stroma are more marked in BD-IPMN with high-grade dysplasia than in that with low-grade dysplasia and are most marked in IPMN with an associated invasive carcinoma.

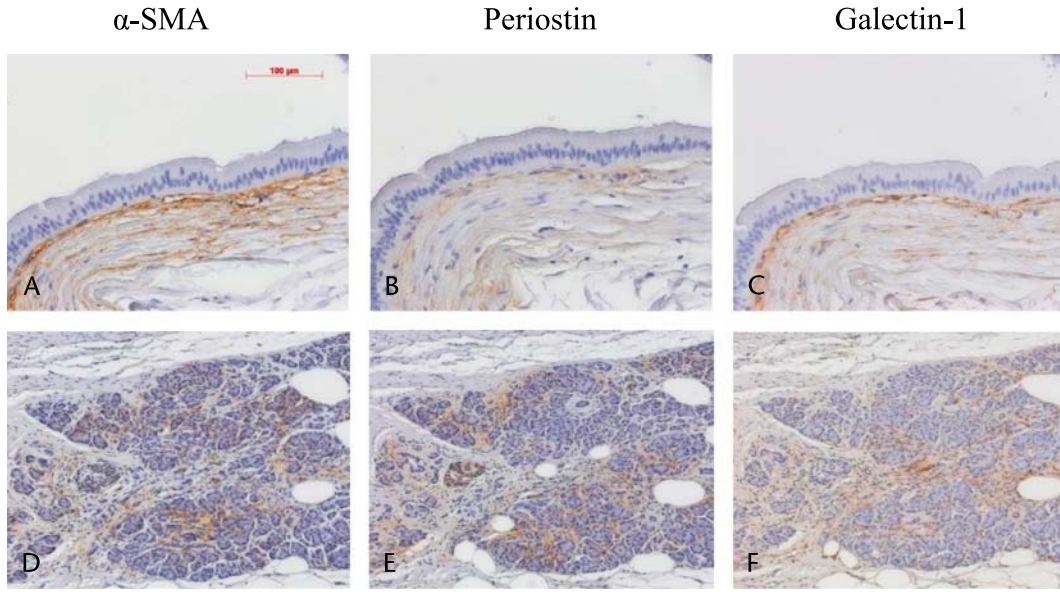

FIGURE 2. Area of positive staining revealed by immunohistochemistry in IPMN. Positive staining of the periductal stroma with anti–α-SMA (A), antiperiostin (B), and antigalectin-1 (C) at a magnification of ×200. Positive staining of the acinar area with anti–α-SMA (D), antiperiostin (E), and antigalectin-1 (F) at a magnification of ×100.

immunoreactivity for periostin and galectin-1 was observed directly beneath the epithelium (Fig. 2A–C). In acinar area, the immunoreactivities for α-SMA, periostin, and galectin-1 were observed at interlobular space (Fig. 2D–F). In BD-IPMN with high-grade dysplasia, the fibrotic band in the stroma surrounding the enlarged pancreatic duct was wider than in BD-IPMN with low-grade dysplasia (Fig. 1B1). Furthermore, immunoreactivity for α-SMA, periostin, and galectin-1 was stronger in BD-IPMN with high-grade dysplasia than in BD-IPMN with low-grade dysplasia (Fig. 1B2–B4).

In MD-IPMN with low-grade dysplasia, the periductal stroma containing fibrosis became more extensive (Fig. 1C1), and

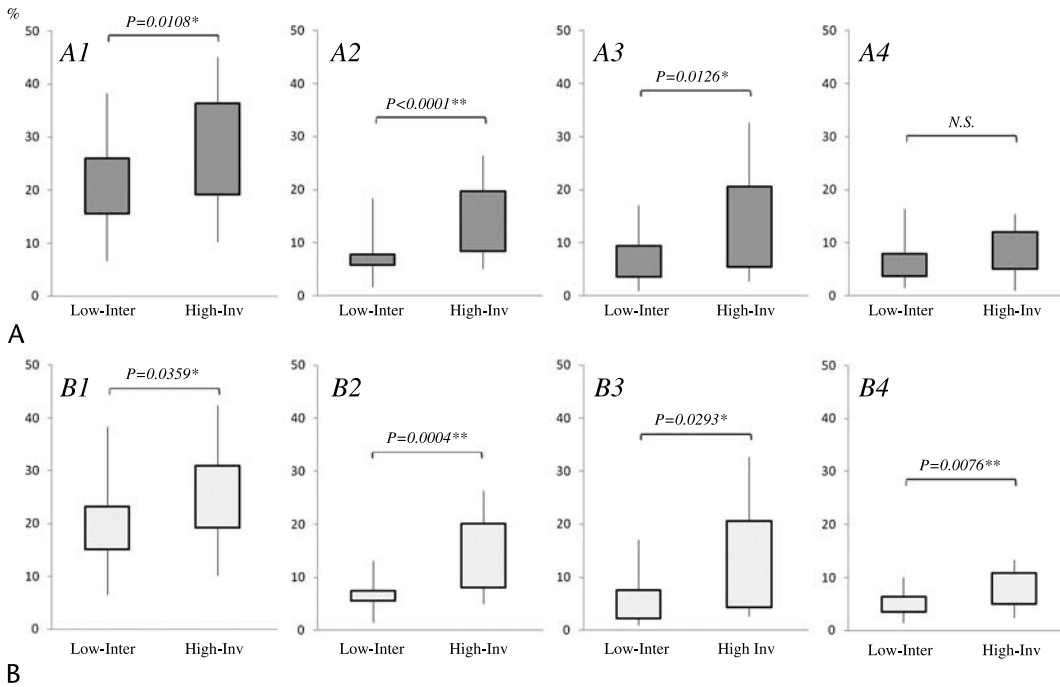

FIGURE 3. Comparison between the low-inter group and the high-inv group. A1–A4, In all IPMN, the degree of fibrosis (A1) and the rates of immunopositivity for α-SMA (A2) and periostin (A3) are significantly higher in the high-inv group than in the low-inter group. Only the rate of immunopositivity for galectin-1 (A4) showed no significant intergroup difference. B1–B4, Within BD-IPMNs, the degree of fibrosis (B1) and the rates of immunopositivity for α-SMA (B2), periostin (B3), and galectin-1 (B4) are significantly higher in the high-inv group than in the low-inter group. The level of statistical significance was set at $*P < 0.05$, $**P < 0.01$.

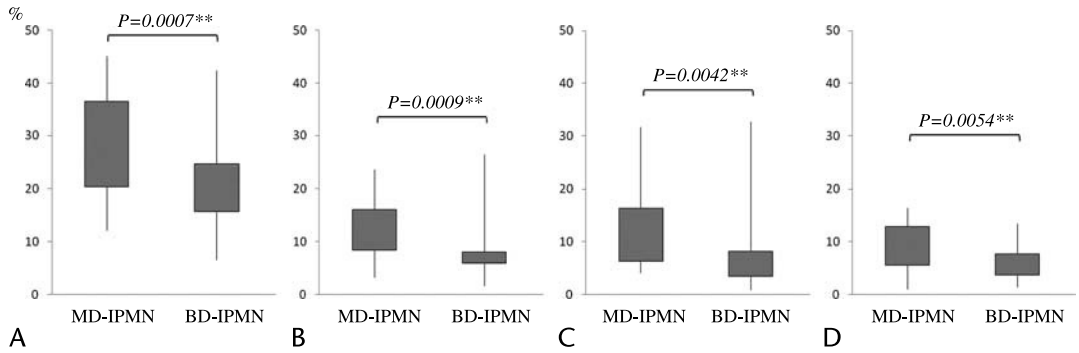

FIGURE 4. Comparison between MD-IPMN and BD-IPMN. The degree of fibrosis (A) and the rates of immunopositivity for α-SMA (B), periostin (C), and galectin-1 (D) are significantly higher in MD-IPMN than in BD-IPMN. The level of statistical significance was set at $^{**}P < 0.01$.

immunoreactivity for α-SMA, periostin, and galectin-1 was stronger than in BD-IPMN with low-grade dysplasia (Fig. 1C2–C4). In MD-IPMN with high-grade dysplasia, stromal fibrosis and immunoreactivity for α-SMA, periostin, and galectin-1 were as more marked than in MD-IPMN with low-grade dysplasia (figure not shown).

In MD-IPMN with an associated invasive carcinoma, stromal fibrosis and immunoreactivity for α-SMA, periostin, and galectin-1 were most marked, similarly to desmoplasia of pancreatic cancer (Fig. 1D1–D4). In BD-IPMN with an associated invasive carcinoma, stromal fibrosis and immunoreactivity were similar to those in MD-IPMN with an associated invasive carcinoma (figure not shown).

Comparison Between the Low-Inter and the High-Inv Groups

The degree of fibrosis and the rates of immunopositivity were compared between the low-inter group and the high-inv group. In comparison of all IPMNs, the degree of fibrosis and the rates of immunopositivity for α-SMA and periostin were significantly higher in the high-inv group than in the low-inter group (Fig. 3A1–A4); the rate of immunopositivity for galectin-1 tended to be higher in the high-inv group but not to be a significant degree. Comparison within the BD-IPMNs demonstrated a significantly higher degree of fibrosis and significantly higher rates of immunopositivity for α-SMA, periostin, and galectin-1 in the high-inv group than in the low-inter group (Fig. 3B1–B4). However, comparison within the MD-IPMNs demonstrated no significant intergroup difference, because the degree of fibrosis and rates of immunopositivity were similarly high in the 2 groups (figure not shown).

Comparison Between MD-IPMN and BD-IPMN

The degree of fibrosis and the rates of immunopositivity were compared between MD-IPMN and BD-IPMN, regardless of histological grade. In comparison of all IPMNs, the degree of fibrosis and rates of immunopositivity for α-SMA, periostin, and galectin-1 were significantly higher in MD-IPMN than in BD-IPMN (Fig. 4A–D).

Univariate Analysis

To clarify the related factors for high-inv group, univariate logistic regression analysis was performed using the degree of fibrosis, rates of immunopositivity, and clinical parameters in all IPMNs. This showed that not only a large cyst diameter, a large MPD diameter, and a large mural nodule, but also a high degree of fibrosis and high rates of immunopositivity for α-SMA and periostin were significant related factors of high-inv group in IPMNs (Table 2). Furthermore, to clarify the indicator of high-inv group with BD-IPMN, univariate logistic regression analysis was performed using those same parameters within the BD-IPMN group. This revealed that a large mural nodule, a high degree of fibrosis, and high rates of immunopositivity for α-SMA, periostin, and galectin-1 were significant related factors of high-inv group with BD-IPMN (Table 3).

Multivariate Analysis

Multivariate logistic regression analysis using MPD diameter, mural nodule size, degree of fibrosis, and rates of immunopositivity (cyst diameter was excluded because the MD-IPMN data were for the mixed type only) indicated that a large mural nodule (odds ratio, 1.228; 95% confidence interval [CI], 1.000–1.507; $P = 0.0496$) and a high rate of immunopositivity for α-SMA (odds ratio, 1.521; 95% CI, 1.110–2.084; $P = 0.0091$) were significant independent related factors for high-inv group in all IPMNs (Table 4). Furthermore, to clarify the indicator of high-inv group with BD-IPMN, multivariate

TABLE 2. Univariate Logistic Regression Analysis Using All IPMNs; Related Factors for the High-Inv Group of IPMN

	Odds Ratio	95% CI	*P*
Age	1.008	0.952–1.067	NS
BMI	1.109	0.973–1.265	NS
Cyst diameter	1.065	1.009–1.124	0.0218*
MPD diameter	1.192	1.018–1.397	0.0296*
Mural nodule size	1.190	1.051–1.348	0.0060†
Serum CEA	1.166	0.928–1.464	NS
Serum CA19-9	1.047	0.997–1.099	NS
Fasting plasma glucose	0.994	0.960–1.031	NS
HbA1c (JPN)	1.179	0.507–2.743	NS
Serum amylase	1.008	0.995–1.021	NS
Serum lipase	1.011	0.990–1.032	NS
Degree of fibrosis	1.083	1.019–1.150	0.0105*
Rate of immunopositivity for α-SMA	1.270	1.109–1.455	0.0006†
Rate of immunopositivity for periostin	1.147	1.050–1.252	0.0022†
Rate of immunopositivity for galectin-1	1.114	0.981–1.264	NS

*$P < 0.05$.

†$P < 0.01$.

CA indicates carbohydrate antigen; CEA, carcinoembryonic antigen; high-inv group, IPMN with high-grade dysplasia and IPMN with an associated invasive carcinoma; NS, not significant.

TABLE 3. Univariate Logistic Regression Analysis Using BD-IPMNs; Related Factors for the High-Inv Group of BD-IPMN

	Odds Ratio	95% CI	*P*
Age	0.979	0.905–1.059	NS
BMI	1.064	0.888–1.275	NS
Cyst diameter	1.057	0.978–1.143	NS
MPD diameter	1.174	0.763–1.806	NS
Mural nodule size	1.299	1.061–1.592	0.0115*
Serum CEA	1.267	0.940–1.709	NS
Serum CA19-9	1.052	0.972–1.138	NS
Fasting plasma glucose	1.003	0.957–1.050	NS
HbA1c (JPN)	0.418	0.091–1.924	NS
Serum amylase	1.015	0.998–1.032	NS
Serum lipase	1.033	0.998–1.070	NS
Degree of fibrosis	1.104	1.004–1.215	0.0414*
Rate of immunopositivity for α-SMA	1.586	1.132–2.224	0.0074†
Rate of immunopositivity for periostin	1.198	1.051–1.367	0.0069†
Rate of immunopositivity for galectin-1	1.447	1.110–1.888	0.0064†

*$P < 0.05$.

†$P < 0.01$.

CA indicates carbohydrate antigen; CEA, carcinoembryonic antigen; high-inv group, IPMN with high-grade dysplasia and IPMN with an associated invasive carcinoma; NS; not significant.

logistic regression analysis was performed using cyst diameter, MPD diameter, mural nodule size, degree of fibrosis, and rates of immunopositivity within BD-IPMNs. This revealed that a large mural nodule (odds ratio, 2.716; 95% CI, 1.006–7.335; $P = 0.0487$) and a high rate of immunopositivity for α-SMA (odds ratio, 13.802; 95% CI, 1.108–171.893; $P = 0.0414$) were significant independent related factors for high-inv group with BD-IPMN (Table 5).

DISCUSSION

It is now more than 30 years since IPMNs were first reported. In Japan, the 5-year survival rate for patients of pancreatic cancer after resection is 18.8%,[24] whereas that for patients of IPMN with an associated invasive carcinoma was 57.7%.[7] Consequently, IPMN is considered to have a better prognosis than pancreatic cancer.[25] A high cure rate is possible if IPMNs are resected before they become invasive.[7] Therefore, the accurate diagnosis of the degree of progression is important. Differentiation between MD-IPMN and BD-IPMN is also an important factor determining operability; however, relevant operability for BD-IPMN is still uncertain. Accordingly, credible predictive factors for BD-IPMN malignancy are urgently needed.

TABLE 4. Multivariate Logistic Regression Analysis Using all IPMNs; Independent Related Factors for the High-Inv Group of IPMN

	Odds Ratio	95% CI	*P*
MPD diameter	1.011	0.821–1.245	NS
Mural nodule size	1.228	1.000–1.507	0.0496*
Degree of fibrosis	0.990	0.882–1.112	NS
Rate of immunopositivity for α-SMA	1.521	1.110–2.084	0.0091†
Rate of immunopositivity for periostin	0.940	0.773–1.143	NS
Rate of immunopositivity for galectin-1	0.834	0.660–1.054	NS

*$P < 0.05$.

†$P < 0.01$.

High-inv group indicates IPMN with high-grade dysplasia and IPMN with an associated invasive carcinoma; NS, not significant.

TABLE 5. Multivariate Logistic Regression Analysis Using BD-IPMNs; Independent Related Factors for the High-Inv Group of BD-IPMN

	Odds Ratio	95% CI	*P*
Cyst diameter	1.225	0.967–1.552	NS
MPD diameter	0.406	0.132–1.250	NS
Mural nodule size	2.716	1.006–7.335	0.0487*
Degree of fibrosis	0.694	0.422–1.143	NS
Rate of immunopositivity for α-SMA	13.802	1.108–171.893	0.0414*
Rate of immunopositivity for periostin	0.763	0.400–1.455	NS
Rate of immunopositivity for galectin-1	1.262	0.644–2.474	NS

*$P < 0.05$.

High-inv group indicates IPMN with high-grade dysplasia and IPMN with an associated invasive carcinoma; NS, not significant.

A large cyst diameter, a large MPD diameter, and a large mural nodule as predictive factors of malignancy have been used for determination of operability at various medical institutions.[10,26,27] Among these characteristics, a large mural nodule is considered to be the most reliable predictive factor.[27,28] The present study is the first to indicate that fibrosis and the expression of matricellular proteins in the periductal stroma are useful for predicting the histological grade of IPMN. Based on these results, the histological grade of IPMN with marked stromal fibrosis is more likely to be high-grade dysplasia or IPMN with an associated invasive carcinoma. If the degree of fibrosis in IPMN could be assessed before surgery, this could become a new indicator for determining whether surgery is indicated.

Recently, magnetic resonance elastography and endoscopic ultrasound elastography have been applied for assessment of pancreatic fibrosis.[29,30] However, the resolution and objectivity of these modalities have been insufficient for precise evaluation. Therefore, new or more developed modalities will be required in the near future.

In the present study, multivariate analysis indicated that a large mural nodule and high α-SMA expression in the periductal stroma were independent related factors in IPMNs with high-grade dysplasia and IPMNs with an associated invasive carcinoma (Tables 4 and 5). Stromal overexpression of α-SMA indicates the presence of activated PSCs and fibroblasts, which may be a critical indicator of the development of pancreatic cancer and malignant IPMNs.

Possible cause of fibrosis is as a sequela of recurrent pancreatitis. In IPMN, acute and chronic pancreatitis are reported to be often present, because of occlusion of the MPD by mucin.[5,7,31] As reported previously, the obstructive pancreatitis showed uniform distribution of interlobular and intralobular fibrosis in caudal side of the obstruction.[32] However, there were IPMN cases with marked fibrosis in the periductal stroma, which showed unremarkable and heterogeneous parenchymal fibrosis in the present study.

Therefore, we focused on the periductal stroma of IPMN. A high degree of fibrosis limited to around the enlarged pancreatic duct only suggests the existence of stromal-epithelial interaction between stromal fibrosis and IPMN. At the stage of a benign lesion, IPMN may interact with the periductal stroma including fibrosis, activated PSC, and fibroblast and lead to the development of malignancy through growth factors and cytokines, either additively or synergistically. In pancreatic intraepithelial neoplasia (PanIN), another precursor lesion of pancreatic ductal adenocarcinoma, the existence of stromal-epithelial interaction has been suggested. As reported previously, the periductal stroma is scant in low-grade PanIN, whereas it is more marked in high-grade PanIN.[33] In mice with induced PanIN, Hingorani et al[34] reported that endogenous expression of $KRAS^{G12D}$ was evident in progenitor cells and that stromal fibrosis was marked in high-grade PanIN. Recently, Shindo et al[35] reported that the presence of stromal fibroblasts showing expression of podoplanin, a known marker of cancer-associated fibroblasts, in the cyst wall was correlated with IPMN progression. These results support the presence of stromal-epithelial interaction in noninvasive lesions such as IPMN and PanIN.

Periostin (osteoblast-specific factor 2 or OSF-2) is a 93.3 kDa secretory protein identified as a cell adhesion protein for preosteoblasts[36–38] and is known to be a marker of activated stromal fibroblasts in tumors.[38] Recently, periostin has been shown to be highly expressed in various types of cancer and to play various roles in promoting cancer progression.[39–42] Periostin is also overexpressed in the stroma of pancreatic cancer and stimulates cancer growth under conditions of serum deprivation and hypoxia in vitro.[20] Recently, Fukushima et al[43] have reported that periostin deposition in the stroma of malignant IPMN was significantly higher than that in benign IPMN. On the basis of reverse transcription–polymerase chain reaction performed by Affymetrix Human Exon microarray (Santa Clara, Calif), Jury et al[44] reported that the level of periostin mRNA in IPMN with high-grade dysplasia and IPMN with an associated invasive carcinoma was dramatically higher than in those with low- and intermediate-grade dysplasia. In the present univariate logistic regression analysis, high expression of periostin in the periductal stroma was a significant related factor in the high-inv group (Tables 2, 3). However, the mechanism responsible for this effect of periostin was unclear.

Galectin-1 is a 29-kDa β-galactoside–binding protein belonging to the galectin family. It exists as a homodimer and contains a 130 amino acid carbohydrate–recognition domain that is a feature of all galectins.[45] Recently, galectin-1 has been reported to promote the progression of various types of cancer.[46–48] Galectin-1 is also overexpressed in the stroma of pancreatic cancer and promotes the proliferation and invasion of pancreatic cancer cells in vitro.[22] Furthermore, galectin-1 stimulates PSC proliferation and collagen synthesis.[49] Interestingly, the expression of galectin-1 has been demonstrated immunohistochemically in the periductal stroma of PanIN.[50] This finding suggests that galectin-1 is involved in the progression of pancreatic cancer. In the present study, the expression of galectin-1 in the periductal stroma in the high-inv group was significantly higher than in the low-inter group within BD-IPMNs (Fig. 3B). However, contrary to expectation, comparison within MD-IPMNs indicated that galectin-1 expression tended to be higher in the low-inter than in the high-inv group, but not to a significant degree. The reason for the conflicting data regarding galectin-1 expression is unclear. Further investigations of the role of matricellular proteins including periostin and galectin-1 in IPMN seem to be desirable.

Interestingly, our study revealed a higher degree of fibrosis and higher expression of α-SMA, periostin, and galectin-1 in MD-IPMNs than in BD-IPMNs (Fig. 4). This result may have been due to be the larger number of low-inter cases in BD-IPMN than in MD-IPMN. However, comparison within the high-inv group indicated that there was no significant difference between MD-IPMN and BD-IPMN regarding the degree of fibrosis and the rates of immunopositivity for α-SMA, periostin, and galectin-1. On the other hand, comparison within the low-inter group indicated a significantly higher degree of fibrosis and significantly higher rates of immunopositivity for α-SMA, periostin, and galectin-1 in MD-IPMN than in BD-IPMN (figure not shown). These differences in microenvironmental factors including fibrosis and expression of matricellular proteins in the periductal stroma in low- and intermediate-grade dysplasia may be correlated with differences in malignancy between MD-IPMN and BD-IPMN.

In conclusion, fibrosis, including the expression of α-SMA, periostin, and galectin-1, in the periductal stroma is significant related factor of BD-IPMN with high-grade dysplasia and BD-IPMN with an associated invasive carcinoma, as demonstrated by univariate analysis. A large mural nodule and a high expression of α-SMA in the periductal stroma are independent related factors of IPMN with high-grade dysplasia and IPMN with an associated invasive carcinoma, as demonstrated by multivariate analysis. If these related factors could be assessed beforehand, they could become new markers for determining the indications for surgery.

ACKNOWLEDGMENTS

The authors thank Junji Yokozawa for technical support and instruction of the experiment.

REFERENCES

1. Ohashi K, Murakami Y, Maruyama M, et al. Four cases of mucin-producing cancer of the pancreas on specific findings of the papilla of Vater. *Prog Dig Endosc*. 1982;20:348–351.
2. Longnecker DS, Adler G, Hruban RH, et al. Intraductal papillary-mucinous neoplasms of the pancreas. In: Hamilton SR, Aaltonen LA, eds. *WHO Classification of Tumors. Pathology and Genetics of Tumors of the Digestive System*. Lyon, IARC Press; 2000:237–241.
3. Sohn TA, Yeo CJ, Cameron JL, et al. Intraductal papillary mucinous neoplasms of the pancreas: an updated experience. *Ann Surg*. 2004;239: 788–797.
4. Adsay NV, Fukushima N, Furukawa T, et al. Intraductal neoplasms of the pancreas. In: Bosman FT, Carneiro H, Hruban RH, et al., eds. *WHO Classification of Tumors of the Digestive System*. 4th ed. Lyon, IARC Press; 2010:304–313.
5. Tanaka M, Kobayashi K, Mizumoto K, et al. Clinical aspects of intraductal papillary mucinous neoplasm of the pancreas. *J Gastroenterol*. 2005;40: 669–675.
6. Japan Pancreas Society. *General Rules for the Study of Pancreatic Cancer*. 6th ed. Tokyo, Japan: Kanehara; 2009.
7. Suzuki Y, Atomi Y, Sugiyama M, et al. Cystic neoplasm of the pancreas: A Japanese multiinstitutional study of intraductal papillary mucinous tumor and mucinous cystic tumor. *Pancreas*. 2004;28:241–246.
8. Nagai K, Doi R, Kida A, et al. Intraductal papillary mucinous neoplasms of the pancreas: clinicopathologic characteristics and long-term follow-up after resection. *World J Surg*. 2008;32:271–278.
9. Tanaka M, Fernández-del Castillo C, Adsay V, et al. International consensus guidelines 2012 for the management of IPMN and MCN of the pancreas. *Pancreatology*. 2012;12:183–197.
10. Sugiyama M, Izumisato Y, Abe N, et al. Predictive factors for malignancy in intraductal papillary-mucinous tumors of the pancreas. *Br J Surg*. 2003; 90:1244–1249.

11. Bachem MG, Schünemann M, Ramadani M, et al. Pancreatic carcinoma cells induce fibrosis by stimulating proliferation and matrix synthesis of stellate cells. *Gastroenterology*. 2005;128:907–921.
12. Omary MB, Lugea A, Lowe AW, et al. The pancreatic stellate cell: a star on the rise in pancreatic diseases. *J Clin Invest*. 2007;117:50–59.
13. Pandol S, Edderkaoui M, Gukovsky I, et al. Desmoplasia of pancreatic ductal adenocarcinoma. *Clin Gastroenterol Hepatol*. 2009;7:S44–S47.
14. Masamune A, Watanabe T, Kikuta K, et al. Roles of pancreatic stellate cells in pancreatic inflammation and fibrosis. *Clin Gastroenterol Hepatol*. 2009; 7:S48–S54.
15. Dunér S, Lopatko Lindman J, Ansari D, et al. Pancreatic cancer: the role of pancreatic stellate cells in tumor progression. *Pancreatology*. 2010;10: 673–681.
16. Bachem MG, Schneider E, Gross H, et al. Identification, culture, and characterization of pancreatic stellate cells in rats and humans. *Gastroenterology*. 1998;115:421–432.
17. Fujita H, Ohuchida K, Mizumoto K, et al. alpha-Smooth muscle actin expressing stroma promotes an aggressive tumor biology in pancreatic ductal adenocarcinoma. *Pancreas*. 2010;39:1254–1262.
18. Togo S, Polanska UM, Horimoto Y, et al. Carcinoma-associated fibroblasts are a promising therapeutic target. *Cancers (Basel)*. 2013;5:149–169.
19. Shindo K, Aishima S, Ohuchida K, et al. Podoplanin expression in cancer-associated fibroblasts enhances tumor progression of invasive ductal carcinoma of the pancreas. *Mol Cancer*. 2013;12:168.
20. Erkan M, Kleeff J, Gorbachevsky A, et al. Periostin creates a tumor-supportive microenvironment in the pancreas by sustaining fibrogenic stellate cell activity. *Gastroenterology*. 2007;132:1447–1464.
21. Kanno A, Satoh K, Masamune A, et al. Periostin, secreted from stromal cells, has biphasic effect on cell migration and correlates with the epithelial to mesenchymal transition of human pancreatic cancer cells. *Int J Cancer*. 2008;122:2707–2718.
22. Masamune A, Satoh M, Hirabayashi J, et al. Galectin-1 induces chemokine production and proliferation in pancreatic stellate cells. *Am J Physiol Gastrointest Liver Physiol*. 2006;290:G729–G736.
23. Xue X, Lu Z, Tang D, et al. Galectin-1 secreted by activated stellate cells in pancreatic ductal adenocarcinoma stroma promotes proliferation and invasion of pancreatic cancer cells. An in vitro study on the microenvironment of pancreatic ductal adenocarcinoma. *Pancreas*. 2011; 40:832–839.
24. Egawa S, Toma H, Ohigashi H, et al. Japan Pancreatic Cancer Registry; 30th year anniversary: Japan Pancreas Society. *Pancreas*. 2012;41:985–992.
25. Sohn TA, Yeo CJ, Cameron JL, et al. Intraductal papillary mucinous neoplasms of the pancreas: an increasingly recognized clinicopathologic entity. *Ann Surg*. 2001;234:313–321.
26. Hirono S, Tani M, Kawai M, et al. Treatment strategy for intraductal papillary mucinous neoplasm of the pancreas based on malignant predictive factors. *Arch Surg*. 2009;144:345–349.
27. Uehara H, Ishikawa O, Katayama K, et al. Size of mural nodule as an indicator of surgery for branch duct intraductal papillary mucinous neoplasm of the pancreas during follow-up. *J Gastroenterol*. 2011;46: 657–663.
28. Schmidt CM, White PB, Waters JA, et al. Intraductal papillary mucinous neoplasms: predictors of malignant and invasive pathology. *Ann Surg*. 2007;246:644–651.
29. Itoh Y, Itoh A, Kawashima H, et al. Quantitative analysis of diagnosing pancreatic fibrosis using EUS-elastography (comparison with surgical specimens). *J Gastroenterol*. 2014;49:1183–1192.
30. Shi Y, Glaser KJ, Venkatesh SK, et al. Feasibility of using 3D MR elastography to determine pancreatic stiffness in healthy volunteers. *J Magn Reson Imaging*. 2015;41:369–375.
31. Ringold DA, Shroff P, Sikka SK, et al. Pancreatitis is frequent among patients with side-branch intraductal papillary mucinous neoplasia diagnosed by EUS. *Gastrointest Endosc*. 2009;70:488–494.
32. Suda K, Mogami M, Oyama T, et al. Histopathological and immunohistochemical studies on alcoholic pancreatitis and chronic obstructive pancreatitis: special emphasis on ductal obstruction and genesis of pancreatitis. *Am J Gastroenterol*. 1990;85:271–276.
33. Korc M. Pancreatic cancer-associated stroma production. *Am J Surg*. 2007; 194:S84–S86.
34. Hingorani SR, Petricoin EF, Maitra A, et al. Preinvasive and invasive ductal pancreatic cancer and its early detection in the mouse. *Cancer Cell*. 2003;4:437–450.
35. Shindo K, Aishima S, Ohuchida K, et al. Podoplanin expression in the cyst wall correlates with the progression of intraductal papillary mucinous neoplasm. *Virchows Arch*. 2014;465:265–273.
36. Takeshita S, Kikuno R, Tezuka K, et al. Osteoblast-specific factor 2: cloning of a putative bone adhesion protein with homology with the insect protein fasciclin I. *Biochem J*. 1993;294(Pt 1):271–278.
37. Horiuchi K, Amizuka N, Takeshita S, et al. Identification and characterization of a novel protein, periostin, with restricted expression to periosteum and periodontal ligament and increased expression by transforming growth factor beta. *J Bone Miner Res*. 1999;14:1239–1249.
38. Morra L, Moch H. Periostin expression and epithelial-mesenchymal transition in cancer: a review and an update. *Virchows Arch*. 2011; 459:465–475.
39. Bao S, Ouyang G, Bai X, et al. Periostin potently promotes metastatic growth of colon cancer by augmenting cell survival via the Akt/PKB pathway. *Cancer Cell*. 2004;5:329–339.
40. Siriwardena BS, Kudo Y, Ogawa I, et al. Periostin is frequently overexpressed and enhances invasion and angiogenesis in oral cancer. *Br J Cancer*. 2006;95:1396–1403.
41. Puglisi F, Puppin C, Pegolo E, et al. Expression of periostin in human breast cancer. *J Clin Pathol*. 2008;61:494–498.
42. Ruan K, Bao S, Ouyang G. The multifaceted role of periostin in tumorigenesis. *Cell Mol Life Sci*. 2009;66:2219–2230.
43. Fukushima N, Kikuchi Y, Nishiyama T, et al. Periostin deposition in the stroma of invasive and intraductal neoplasms of the pancreas. *Mod Pathol*. 2008;21:1044–1053.
44. Jury RP, Thibodeau BJ, Fortier LE, et al. Gene expression changes associated with the progression of intraductal papillary mucinous neoplasms. *Pancreas*. 2012;41:611–618.
45. Camby I, Le Mercier M, Lefranc F, et al. Galectin-1: a small protein with major functions. *Glycobiology*. 2006;16:137R–157R.
46. Zhao XY, Chen TT, Guo M, et al. Hypoxia inducible factor-1 mediates expression of galectin-1: the potential role in migration/invasion of colorectal cancer cells. *Carcinogenesis*. 2010;31:1367–1375.
47. van den Brûle FA, Waltregny D, Castronovo V. Increased expression of galectin-1 in carcinoma-associated stroma predicts poor outcome in prostate carcinoma patients. *J Pathol*. 2001;193:80–87.
48. van den Brule F, Califice S, Garnier F, et al. Galectin-1 accumulation in the ovary carcinoma peritumoral stroma is induced by ovary carcinoma cells and affects both cancer cell proliferation and adhesion to laminin-1 and fibronectin. *Lab Invest*. 2003;83:377–386.
49. Fitzner B, Walzel H, Sparmann G, et al. Galectin-1 is an inductor of pancreatic stellate cell activation. *Cell Signal*. 2005;17:1240–1247.
50. Pan S, Chen R, Reimel BA, et al. Quantitative proteomics investigation of pancreatic intraepithelial neoplasia. *Electrophoresis*. 2009;30: 1132–1144.